

# Physical Properties of Hybrid Nanofluids with Various Models

Hemavathi P, Vijaya Kumar Reddy K

Department of Mechanical Engineering, JNTUH College of Engineering, Hyderabad  
Email: hhemapattu8@gmail.com

This study examines the thermophysical properties of graphene oxide (GO),  $\text{SiO}_2$ , and  $\text{TiO}_2$  nanofluids, focusing on thermal conductivity and dynamic viscosity. Theoretical models like Wasp, Maxwell, and Brinkman were compared with experimental data. GO showed the highest thermal conductivity, especially in experimental settings, due to its unique properties. Theoretical models tended to underestimate thermal conductivity and overestimate viscosity. These findings indicate that GO nanofluids hold potential for applications requiring efficient heat transfer.

**Keywords:** Heat Transfer, hybrid nanofluids, Physical properties.

## 1. Introduction

Nanofluids, which involve the suspension of nanoparticles in base fluids, are emerging as promising solutions for enhancing heat transfer in heat exchangers. By improving the thermal properties of fluids, nanofluids could lead to more efficient designs and processes. Despite their potential, challenges remain in optimizing these fluids for industrial use, especially concerning long-term stability and the balance between performance and design complexity.

## 2. Literature Review:

Wong et al. (2021) reported a 25% increase in heat transfer using Cu-Graphene hybrid nanofluids in a shell-and-tube heat exchanger (STHE), highlighting the enhanced thermal conductivity and stability of hybrid nanofluids for continuous operations. Patel and Sahu (2022) demonstrated a 30% improvement in heat transfer with  $\text{SiO}_2$ - $\text{Al}_2\text{O}_3$  hybrid nanofluids, attributing the increase to better energy distribution and minimized boundary layers. Li et al. (2020) found that spherical nanoparticles, particularly  $\text{Al}_2\text{O}_3$ - $\text{SiO}_2$  combinations, offer superior thermal conductivity and reduced pressure drops due to more uniform fluid distribution compared to rod-shaped particles. As et al. (2021) observed a 20% enhancement in heat transfer in turbulent flows with  $\text{CuO}$ - $\text{SiO}_2$  hybrid nanofluids, citing the unique properties of

the hybrid composition. Jadhav et al. (2020) reported a 20% increase in thermal conductivity for CuO-TiO<sub>2</sub> hybrid nanofluids compared to CuO-water nanofluids. Khan and Ahmad (2022) noted that hybrid nanofluids displayed better suspension stability and reduced nanoparticle agglomeration, leading to more consistent heat transfer over time. Singh et al. (2021) showed that the viscosity of hybrid nanofluids, particularly Cu-Graphene mixtures, can be optimized to reduce pressure drops. Kumar et al. (2021) emphasized that hybrid nanofluids containing graphene oxide (GO) and TiO<sub>2</sub> improved heat transfer by 30%, despite an increase in viscosity at higher concentrations. Esfe et al. (2018) demonstrated a 28% enhancement in thermal conductivity with SiO<sub>2</sub>-TiO<sub>2</sub> hybrid nanofluids, noting the balance between efficiency and stability in STHEs. Suresh et al. (2020) and Putra et al. (2016) highlighted the improved heat transfer and energy absorption in natural convection systems using hybrid nanofluids, although they emphasized the need for stabilizers to mitigate nanoparticle sedimentation. Oztop et al. (2015) observed that SiO<sub>2</sub>-TiO<sub>2</sub> hybrid nanofluids improved buoyancy-driven natural convection due to their slightly higher density.

Collectively, these studies demonstrate that hybrid nanofluids enhance heat transfer performance through improved thermal conductivity, stability, and reduced nanoparticle agglomeration, with nanoparticle selection playing a critical role in optimizing performance.

### **3. Experimental work and Methodology:**

To effectively predict the heat transfer behaviour of nanofluids (NFs), it's crucial to understand their thermophysical properties. Adding nanoparticles (NPs) to conventional working fluids significantly alters these properties, enhancing heat transfer performance. Key thermophysical properties of nanofluids include:

1. Thermal Conductivity: NPs typically improve the thermal conductivity of base fluids (BFs). This enhancement depends on the size, shape, and material of the nanoparticles, leading to better heat transfer.
2. Viscosity: The viscosity of nanofluids can increase or decrease based on NP concentration and characteristics. Higher viscosity may hinder fluid flow, affecting convective heat transfer, so finding a balance is essential.
3. Specific Heat Capacity: The presence of NPs can alter the specific heat capacity of nanofluids, influencing their ability to store and transfer thermal energy. An increase can be beneficial for thermal energy storage applications.
4. Density: Nanofluids generally have higher density than their base fluids, influenced by NP type and concentration. Changes in density can impact buoyancy-driven flow and overall heat transfer.

Several factors influence the thermophysical properties of nanofluids:

- Nanoparticle Size and Shape: Smaller NPs with higher surface areas enhance heat transfer by increasing interactions with the base fluid.
- Concentration of NPs: The concentration directly affects nanofluid properties; optimal levels can maximize heat transfer efficiency without excessively increasing viscosity.

- Type of Nanoparticles: Different materials (metals, oxides, carbon-based) exhibit varying thermal conductivities and stabilities, affecting overall performance.
- Base Fluid Properties: The inherent characteristics of the base fluid, such as thermal conductivity, viscosity, and specific heat capacity, are critical in determining nanofluid behaviour.

### Thermal Conductivity Measurements Overview

Current methods for measuring thermal conductivity can be classified into two main categories:

#### Steady State Methods and Transient State Methods.

- Steady State Methods include:
  - a) Parallel Plate Method      b) Coaxial Cylinders Method
- Transient State Methods encompass:
  - a) Transient Hot Wire Method      b) Transient Plane Source Theory
  - c) Temperature Oscillation Method      d) Laser Flash Method      e)  $3\omega$  Method

#### Steady State Methods:

##### a. Parallel Plate Method

In this approach, the sample is placed between two copper parallel plates equipped with thermocouples. One plate is heated, and the temperature difference between the plates is used to determine thermal conductivity. To ensure uniform thickness and reduce convection due to gravity, both plates can be levelled during the loading of the sample.

##### b. Coaxial Cylinders Method

This technique calculates the thermal conductivity of the nanofluid in the annular gap between coaxial cylinders by applying the Fourier equation in cylindrical coordinates. The method reduces natural convection by using minimal temperature gradients. These measurement techniques provide valuable insights into the thermal properties of nanofluids, facilitating advancements in their application for heat transfer enhancements.

#### Transient State Methods:

##### a. Transient Hot Wire Method

In this technique, a thin metal wire (commonly platinum or tantalum) serves as both the heat source and sensor. The wire is submerged in the nanofluid, and a voltage is applied, causing the wire to heat up. The heat transfers to the surrounding liquid, with the rate of transfer depending on the liquid's thermal conductivity. Resistance changes in the wire correlate with temperature variations, allowing for thermal conductivity calculations. Systematic errors, such as those from natural convection, can be corrected experimentally.

##### b. Transient Plane Source Theory

This technique operates similarly to the transient hot wire method but uses a hot disk instead

of a wire. The time variation of the disk's electrical resistance is recorded to calculate thermal conductivity. As with the transient hot wire method, convection currents in the fluid can affect measurements.

#### c. Temperature Oscillation Method

In this method, a cylinder filled with the fluid has oscillating temperatures applied at both ends. The amplitude and phase of the temperature oscillation at the center are measured. To minimize interference from convection, the amplitude of the applied oscillation should be kept as low as possible.

#### d. Laser Flash Method

This method heats the bottom of the fluid sample using a laser, while the temperature at the top is measured with a thermometer. The temperature increase is correlated with thermal conductivity. The rapid heating (on the order of nanoseconds) minimizes the effects of radiation and convection.

#### e. $3\omega$ Method

A metal heater within the fluid is subjected to a sinusoidal electric current at angular frequency  $\omega$ , creating temperature oscillations in the fluid. This frequency is then correlated with the nanofluid's thermal conductivity. This method requires small sample volumes and is particularly suitable for non-spherical particles, such as nanotubes and nanowires, though it takes longer to yield results compared to other techniques.

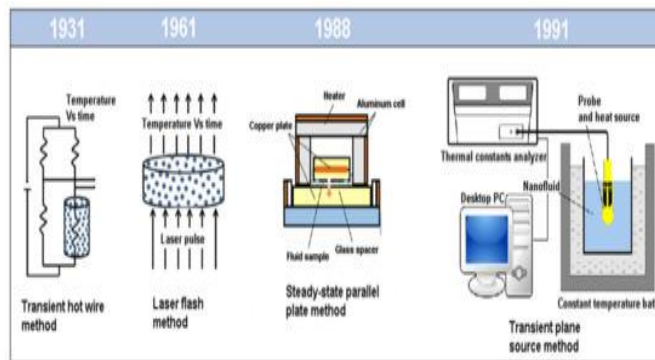


Fig. 1: Schematic diagram of steady and transient state methods to measure the thermal conductivity of nanofluids (NFs)

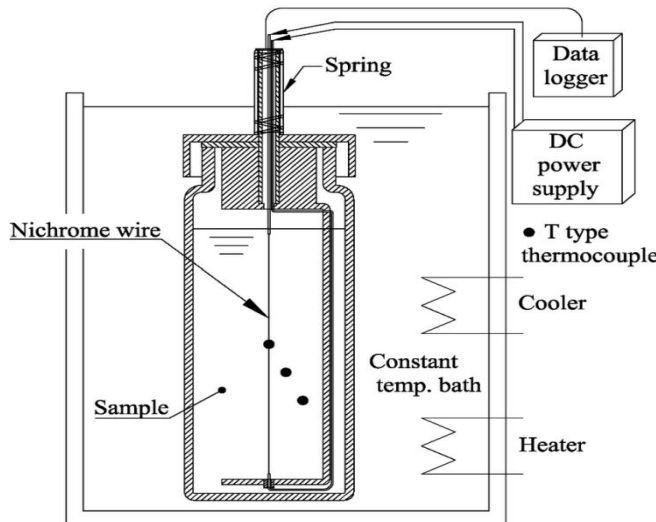


Fig. 2: Thermal conductivity measurement apparatus: transient hot-wire method

#### Viscosity Measurement of Nanofluids:

Fig. 3 illustrates the experimental setup used for viscosity measurements of the nanofluids. A key limitation of this instrument is its low torque performance, which can be affected by friction between the rotating and stationary components. Additionally, the temperature of the tested fluids was controlled between  $-20^{\circ}\text{C}$  and  $70^{\circ}\text{C}$  using a combined motor and transducer (CMT) water circulator chamber. This setup ensures precise control over the testing environment, facilitating accurate viscosity measurements.

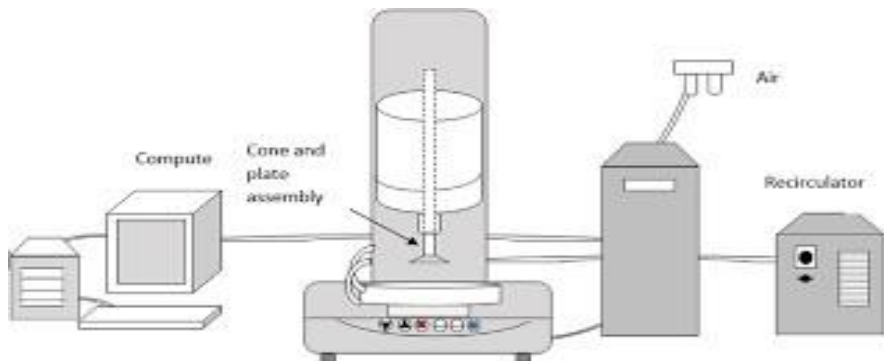


Fig. 3: Viscosity measurement of nanofluids - Experimental setup schematic

#### Density of nanoparticles:

The density of nanoparticles was determined by dividing the mass of the nanoparticles by their volume in a cylindrical beaker containing a solvent (thinner). The composite theoretical density ( $\rho_{th}$ ) was computed utilizing the rule of mixture (ROM) by the below eq.

$$\rho_{th} = V_p \rho_p + V_e \rho_e$$

Where,  $V_p$ ,  $V_e$ ,  $\rho_p$ , and  $\rho_e$  are the volume fraction, the density of nanoparticles and epoxy

matrix, respectively.

The density of the epoxy and the functionally graded polymer nanocomposite samples was experimentally determined using Archimedes' principle. The density of the composites was then calculated using the following equation:

$$\rho_c = \frac{W_a}{W_a + W_w}$$

Where,  $\rho_c$  is the composite density,  $W_a$  and  $W_w$  are the sample weights in air and in water, respectively.

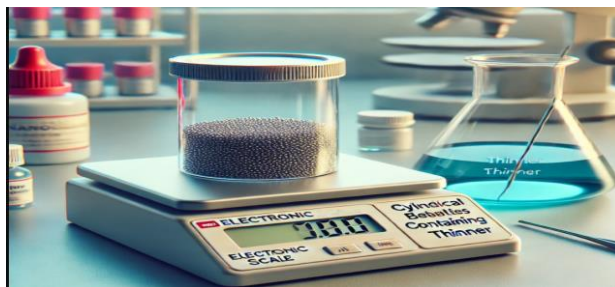


Fig. 4: Measure of density for nanoparticles

Specific heat ( $C_p$ ):

The specific heat for each nanofluid was measured in a Differential Scanning Calorimeter (DSC). The calculation of the specific heat capacity is based in the DIN standard (DIN 51007). The specific heat of nanofluids has been widely predicted using these two phenomenological models.

Model (I): relates the specific heat of the nanofluid to the combined specific heats of its constituents based on the rule of mixtures, expressed as:

$$c_{p,nf} = c_p (1 - \phi) + c_{p,bf} \phi \quad (1)$$

Model (II): assuming thermal equilibrium between the dispersed nanoparticles and liquid phases, the specific heat capacity can be approximated by the expression given by

$$c_{p,nf} = \frac{\phi \rho c_{p,nf} + (1 - \phi) \rho c_{p,bf}}{\phi \rho + (1 - \phi) \rho_{bf}} \quad (2)$$

Where,  $c_p$  is the specific heat,  $\phi$  is the particle volume concentration, and  $\rho$  is the density. The subscripts nf, p, and f denotes nanofluid, particle, and the base fluid, respectively.

The heat transfer rate of nanofluids (NFs) is largely determined by their specific heat capacity ( $C_p$ ). Nanofluids are suspensions of nanoparticles (NPs) dispersed in a base fluid (BF). Several factors influence the ( $C_p$ ) of nanofluids, including the type, concentration, size, and shape of the nanoparticles, as well as the properties of the base fluid. One significant effect of adding nanoparticles to the base fluid is the increased thermal conductivity of the nanofluid, which can result in higher ( $C_p$ ) values compared to the base fluid alone.

#### 4. Data reduction

The thermophysical properties equations are taken from heat and mass transfer design data book [184], and listed in this section.

$$\rho_h = 27 \times 10^{-4} T^2 - 0.1508T + 1003.2 \frac{kg}{m^3} \quad (1)$$

$$\rho_h = 1004.91 \frac{kg}{m^3}$$

$$C_{p,h} = 5 \times 10^{-11} T^6 - 4 \times 10^{-8} T^5 + 1 \times 10^{-5} T^4 - 17 \times 10^{-4} T^3 + 0.128 T^2 - 4.0717 T + 4217.5 \frac{J}{kg.K} \quad (2)$$

(2)

$$C_{p,h} = 4161.97 \frac{J}{kg.K}$$

$$k_h = 8 \times 10^{-11} T^4 + 5 \times 10^{-8} T^3 - 2 \times 10^{-5} T^2 + 25 \times 10^{-4} T + 0.5525 \frac{W}{mK} \quad (3)$$

$$k_h = 0.643040619 \frac{W}{m.K}$$

$$\mu_h = 3 \times 10^{-17} T^6 - 3 \times 10^{-14} T^5 + 2 \times 10^{-11} T^4 - 4 \times 10^{-9} T^3 + 5 \times 10^{-7} T^2 - 4 \times 10^{-5} T + 0.0016$$

$$(4) \mu_h = 0.00033516 \text{ Pa.s}$$

$$\rho_c = 27 \times 10^{-4} T^2 - 0.1508T + 1003.2 \frac{kg}{m^3} \quad (5)$$

$$\rho_c = 1001.16 \frac{kg}{m^3}$$

$$C_{p,c} = 5 \times 10^{-11} T^6 - 4 \times 10^{-8} T^5 + 1 \times 10^{-5} T^4 - 17 \times 10^{-4} T^3 + 0.128 T^2 - 4.0717 T + 4217.5 \frac{J}{kg.K} \quad (6)$$

$$\frac{J}{m.K} \quad C_{p,c} = 4150.15 \frac{J}{kg.K}$$

$$k_c = 8 \times 10^{-11} T^4 + 5 \times 10^{-8} T^3 - 2 \times 10^{-5} T^2 + 25 \times 10^{-4} T + 0.5525 \frac{W}{mK} \quad (7)$$

$$k_c = 0.614658352 \frac{W}{m.K}$$

$$\mu_c = 3 \times 10^{-17} T^6 - 3 \times 10^{-14} T^5 + 2 \times 10^{-11} T^4 - 4 \times 10^{-9} T^3 + 5 \times 10^{-7} T^2 - 4 \times 10^{-5} T + 0.0016$$

$$\mu_c = 0.000706773 \text{ Pa.s}$$

Table 1: Thermophysical Properties of Nanofluids and Base Fluids

| Property                                   | Formula / Model   | Explanation / Key Variables  | Eqn. No       |
|--|---|--|---------------|
| Density ( $\rho_{nf}$ )                    | $\rho_{nf} = (1 - \phi)\rho_{bf} + \phi\rho_p$                                | $\rho_p$ : Density of nano particle<br>$\rho_f$ : base fluid density                                 | 8             |
| Specific Heat ( $C_p$ ) <sub>nf</sub>      | $(C_p)_{nf} = \frac{(1 - \phi)(\rho C_p)_f + \phi(\rho C_p)_{np}}{\rho_{nf}}$ | $c_p$ : Specific heat of particles,<br>$c_f$ : base fluid,   | 9             |
| Thermal Conductivity ( $k$ ) <sub>nf</sub> | Derived from Maxwell and Wasp models (13)                                     | $\phi$ : nanoparticle volume fraction,<br>$k_p, k_f$ : thermal conductivities of particles and fluid | 10            |
| Viscosity ( $\mu$ ) <sub>nf</sub>          | Einstein (14), Brinkman (15), VST models (16-18)                              | $\mu_{nf}$ : viscosity of nanofluid, $\mu_{bf}$ : viscosity of base fluid                            | 11,16, 17, 18 |

Table 2: Evaluation of Viscosity and Thermal Conductivity Models

| Model                      | Property  | Formula/ Model  | Key Factors/Variables                        | Eq |
|----------------------------|-----------|---|--|----|
| Maxwell-Wasp Model         | TC        | $k_{nf} = k_c \left[ \frac{(k_p + ((n-1)k_c) + ((n-1)\phi(k_p - k_c))}{(k_p + ((n-1)k_c) - (\phi(k_p - k_c)))} \right]$ | For spherical particles, n=3                 | 13 |
| Einstein Model             | Viscosity | $\mu_{nf} = \mu_c(1 + 2.5\phi)$   | Used for dilute suspensions                  | 14 |
| Brinkman Equation          | Viscosity | $\frac{\mu_{nf}}{\mu_{bf}} = 1.453 \left(1 + \frac{T}{60}\right)^{-0.2165} \left(1 + \frac{\phi}{100}\right)^{79.10}$   | General case                                 | 15 |
| VST of GO-SiO <sub>2</sub> | Viscosity | $\frac{\mu_{nf}}{\mu_{bf}} = 1.475 \left(1 + \frac{T}{60}\right)^{-0.3899} \left(1 + \frac{\phi}{100}\right)^{66.97}$   | Viscosity for GO-SiO <sub>2</sub> nanofluid  | 17 |
| VST of GO-TiO <sub>2</sub> | Viscosity | $\frac{\mu_{nf}}{\mu_{bf}} = 1.483 \left(1 + \frac{T}{60}\right)^{-0.3399} \left(1 + \frac{\phi}{100}\right)^{71.45}$   | Viscosity for GO-TiO <sub>2</sub> nanofluid  | 18 |
| TC of GO                   | TC        | $\frac{k_{nf}}{k_{bf}} = 0.9263 \left(1 + \frac{T}{60}\right)^{0.2787} \left(1 + \frac{\phi}{100}\right)^{30.38}$       | Thermal conductivity for GO                  | 19 |
| TC of GO-SiO <sub>2</sub>  | TC        | $\frac{k_{nf}}{k_{bf}} = 0.8356 \left(1 + \frac{T}{60}\right)^{0.3937} \left(1 + \frac{\phi}{100}\right)^{22.34}$       | Thermal conductivity for GO-SiO <sub>2</sub> | 20 |
| TC of GO-TiO <sub>2</sub>  | TC        | $\frac{k_{nf}}{k_{bf}} = 0.8441 \left(1 + \frac{T}{60}\right)^{0.3991} \left(1 + \frac{\phi}{100}\right)^{23.26}$       | Thermal conductivity for GO-TiO <sub>2</sub> | 21 |

## 5. Experimental Results:

Table 3: Thermal conductivity of various models

| Model            | Wasp model   | Maxwell model   | Praveen Kanti et al.  |
|------------------|--|---|---|
|                  | $knf = kc \{ (kp + ((n-1)kc) + ((n-1)\phi(kp-kc)) / (kp + ((n-1)kc) - (\phi(kp-kc))) \}$ | $knf = kc \{ (knp + 2kc + 2\phi(knp-kc)) / (knp + 2kc - \phi(knp-kc)) \}$ | $knf = 0.9263kbf \{ 1 + [T/60] \}^{0.2787} \{ 1 + [\phi/100] \}^{30.38} \}$ |
| GO               | 0.63347  | 0.63347   | 0.97421   |
|                  | 0.67187  | 0.67187   | 1.03956   |
|                  | 0.71189  | 0.71189   | 1.10819   |
| SiO <sub>2</sub> | 0.62037  | 0.62037   | 1.66258   |
|                  | 0.63151  | 0.63151   | 1.78205   |
|                  | 0.64280  | 0.64280   | 1.90820   |
| TiO <sub>2</sub> | 0.62988  | 0.62988   | 1.67905   |
|                  | 0.66069  | 0.66069   | 1.80003   |
|                  | 0.69255  | 0.69255   | 1.92781   |

Table 4: Dynamic viscosity

| Model            | Einstein eqn.                   | Brinkman eqn.                         | Praveen Kanti et al.   |
|------------------|---------------------------------|---------------------------------------|--|
|                  | $\mu_{nf} = \mu_c(1 + 2.5\phi)$ | $\mu_{nf} = \mu_c / (1 - \phi)^{2.5}$ | $\mu_{nf} = 1.453\mu_{bf} \{ 1 + (T/60) \}^{0.2165} \{ 1 + (\phi/100) \}^{79.10} \}$ |
| GO               | 0.000724                        | 0.000725                              | 0.000717   |
|                  | 0.000760                        | 0.000763                              | 0.000764   |
|                  | 0.000795                        | 0.000803                              | 0.000813   |
| SiO <sub>2</sub> | 0.000724                        | 0.000725                              | 0.000526   |
|                  | 0.000760                        | 0.000763                              | 0.000568   |
|                  | 0.000795                        | 0.000803                              | 0.000612   |
| TiO <sub>2</sub> | 0.000724                        | 0.000725                              | 0.000576   |
|                  | 0.000760                        | 0.000763                              | 0.000623   |
|                  | 0.000795                        | 0.000803                              | 0.000672   |

$knf$ : Thermal conductivity of nanofluid,  $kc$  /  $kbf$ : Thermal conductivity of the base fluid,

$kp$  /  $knp$ : Thermal conductivity of the nanoparticles,  $n$ : Shape factor of the nanoparticles,

$\phi$ : Volume fraction of nanoparticles,  $T$ : Temperature of the nanofluid (only in the Praveen Kanti model),  $\mu_{nf}$ : Effective viscosity of the nanofluid,  $\mu_c$  /  $\mu_{bf}$ : Viscosity of the base fluid.

## 6. Results and discussion

In this section author is going to discuss the physical properties of nanofluids based on various models for various nanofluids.

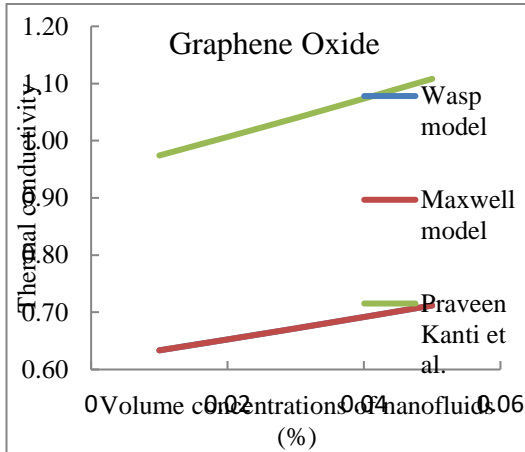


Fig. 1: Thermal conductivity of GO

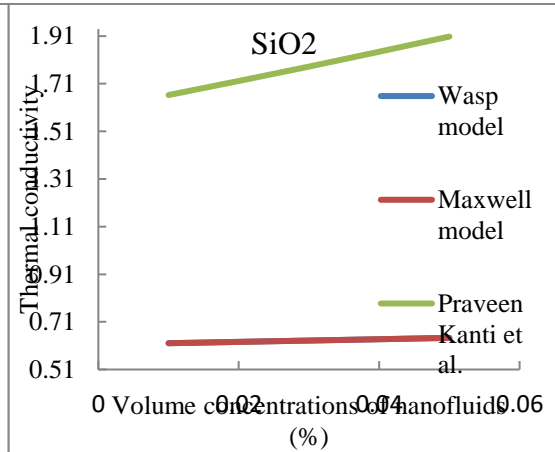
Fig. 2: Thermal conductivity of SiO<sub>2</sub>

Fig. 1 shows that increasing GO nanofluid concentrations greatly enhance thermal conductivity, with the Wasp model predicting the highest improvement, highlighting GO's potential in thermal applications.

In Fig. 2, both Wasp and Maxwell models show minimal changes for SiO<sub>2</sub> nanofluid conductivity, while experimental data from Praveen Kanti et al. reveal larger increases, exposing a gap between theoretical predictions and experimental outcomes.

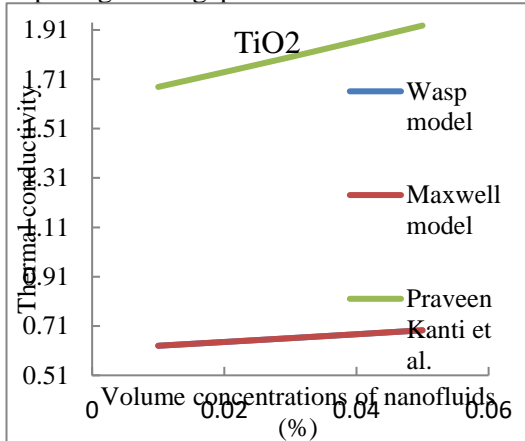
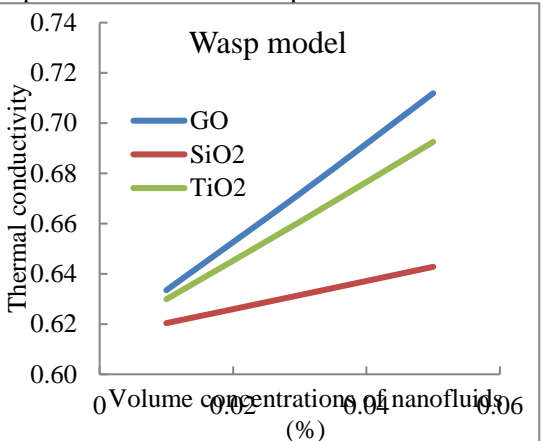
Fig. 3: Thermal conductivity of TiO<sub>2</sub>

Fig. 4: Thermal conductivity of various nanofluids based on Wasp model

In Fig. 3, the Wasp and Maxwell models show minimal changes in TiO<sub>2</sub> nanofluid conductivity with increased concentrations, while Praveen Kanti et al. report a significant increase, indicating a more dynamic relationship. Fig. 4 reveals the Wasp model predicts the highest conductivity for graphene oxide nanofluids, with silicon dioxide showing the least improvement, while all nanofluids exhibit a linear increase in conductivity with rising volume concentration.

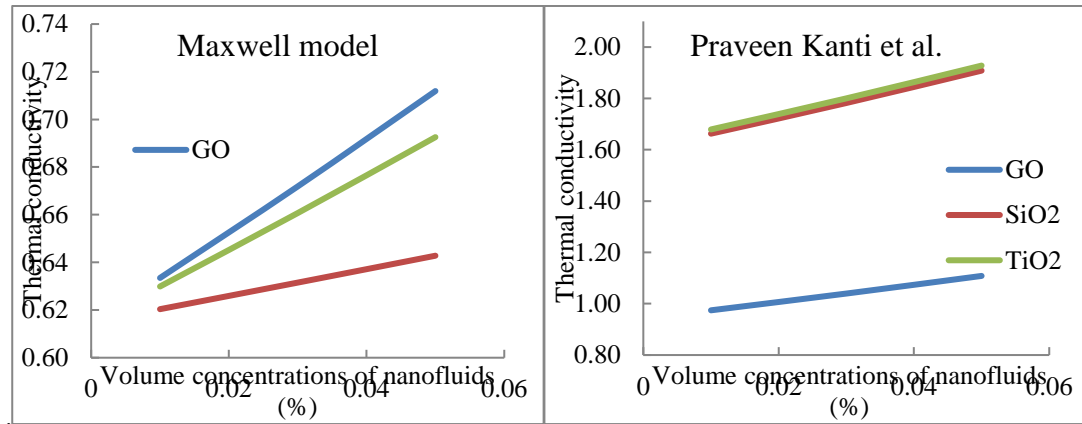


Fig. 5: Thermal conductivity of various nanofluids based on Maxwell model

Fig. 6: Thermal conductivity of various nanofluids based on Praveen Kanti et al. model

In Fig. 5, both models show graphene oxide outperforming the other nanofluids, while silicon dioxide has the least effect on thermal conductivity. However, in Fig. 6, Praveen Kanti et al.'s model shows TiO<sub>2</sub> and SiO<sub>2</sub> outperforming GO across all concentrations, highlighting how different models yield varying predictions of nanofluid behavior.

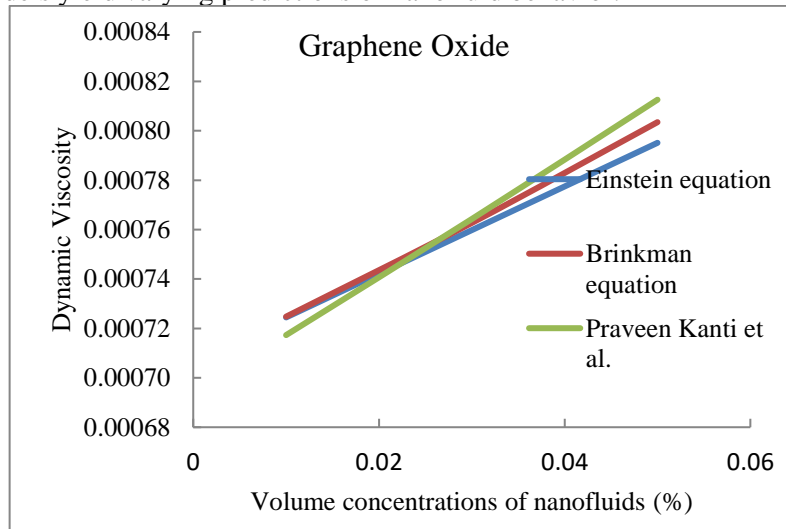


Fig. 7: Thermal conductivity of GO for various models

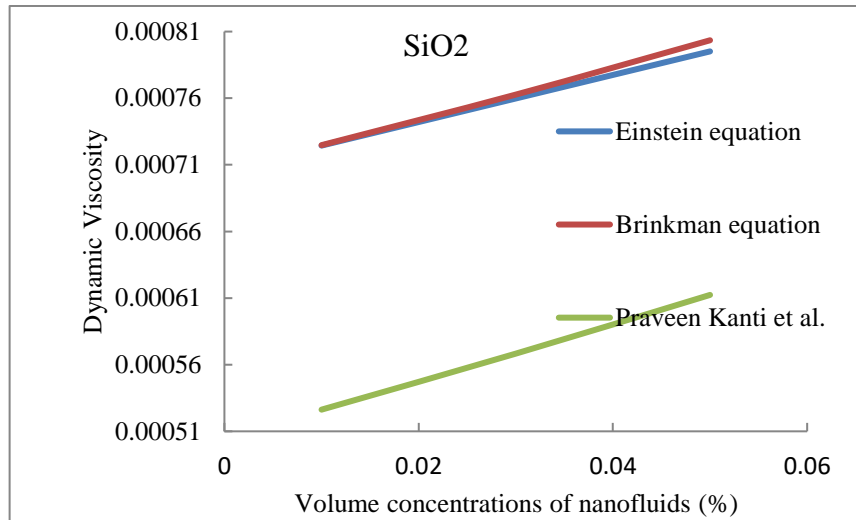
Fig. 8: Dynamic Viscosity of SiO<sub>2</sub> for various models

Fig. 7 shows all models predicting a linear increase in graphene oxide nanofluid viscosity with concentration. The Brinkman equation gives slightly higher values, while experimental data by Praveen Kanti et al. fall between the models, reflecting real-world factors.

In Fig. 8, both the Einstein and Brinkman equations overestimate the viscosity of SiO<sub>2</sub> nanofluids, with experimental results showing lower values, indicating the models may overpredict the impact of concentration on viscosity.

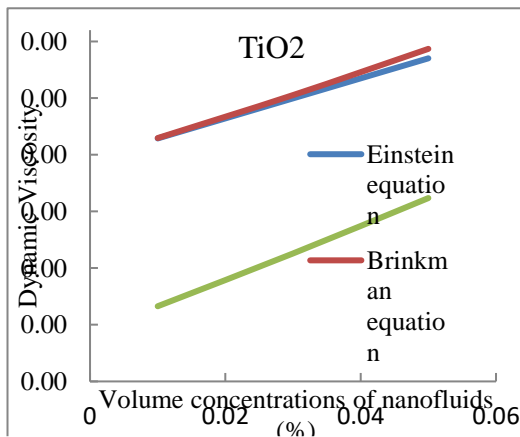
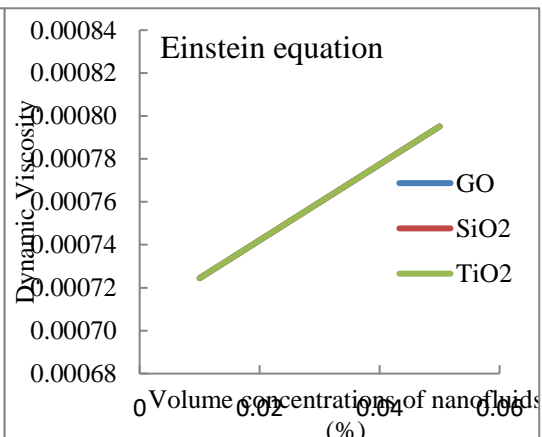
Fig. 9: Dynamic Viscosity of TiO<sub>2</sub> for various models

Fig.10: Dynamic Viscosity of Einstein equation for various nanofluids model

Fig. 9 shows that dynamic viscosity for TiO<sub>2</sub> nanofluids increases with concentration, with theoretical predictions reaching about 0.00081 at 0.06%, while Praveen Kanti et al. report lower viscosities (0.00050 to 0.00062), suggesting potential model overestimation. Fig. 10 indicates that the Einstein equation predicts a linear viscosity increase for all three nanofluids, emphasizing TiO<sub>2</sub>'s greater impact on viscosity.

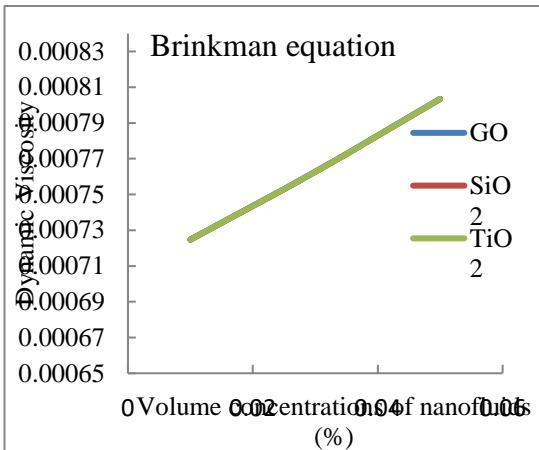


Fig. 11: Dynamic Viscosity of Brinkman equation for various nanofluids

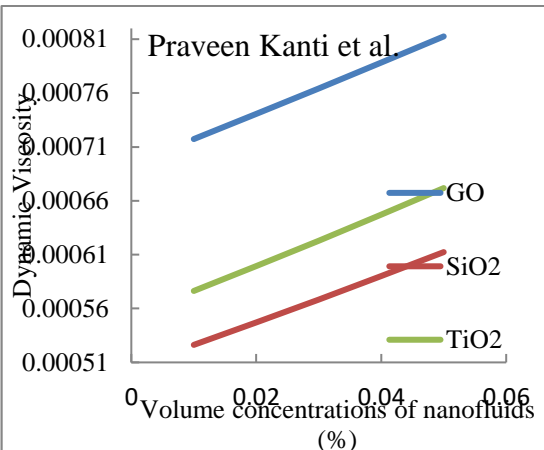


Fig. 12: Dynamic Viscosity of Praveen Kanti et al. equation for various nanofluids

Fig. 11 shows that higher nanoparticle concentrations increase viscosity, with TiO<sub>2</sub> contributing the most to thickening, followed by SiO<sub>2</sub> and GO.

Fig. 12 suggests that GO has a stronger impact on viscosity than TiO<sub>2</sub> and SiO<sub>2</sub>, due to differences in nanoparticle properties and interactions with the base fluid, emphasizing the significant role of nanoparticle type in influencing viscosity.

## 7. Conclusion:

Graphene oxide nanofluids exhibit superior thermal conductivity, making them highly suitable for heat transfer applications. However, the models used in this study—such as Wasp, Maxwell, and Brinkman—tend to underestimate real-world performance, highlighting the need for further research into nanoparticle behavior and interactions. Overall, the study suggests that hybrid nanofluids, particularly those containing GO, hold strong potential for improving the efficiency of thermal systems.

## References

1. Wong S.W(2021), "Cu-Graphene Water-Based Hybrid Nanofluids: Synthesis, Stability, Thermophysical Characterization, and Figure of Merit Analysis", *Journal of Thermal Analysis and Calorimetry*, Springer, DOI:10.1007/s10973-021-10542-w.
2. Patel and Sahu (2022), "Heat transfer performance of SiO<sub>2</sub>-Al<sub>2</sub>O<sub>3</sub> hybrid nanofluids in shell-and-tube heat exchangers (STHE)", *International Journal of Thermophysics*, Springer, DOI: 10.1007/s10765-022-03078-x.
3. Li Y, Wang X, Chen Y, Zhao Y, "Performance of Spherical Nanoparticles in Hybrid Nanofluids: A Comparative Study of Al<sub>2</sub>O<sub>3</sub>-SiO<sub>2</sub> Combinations", *Journal of Nanoscience and Nanotechnology*, DOI: 10.1166/jnn.2020.17773.
4. As S, Kumar R, Singh P, Yadav A, "Performance Evaluation of CuO-SiO<sub>2</sub> Hybrid Nanofluids in Shell-and-Tube Heat Exchangers", *Journal of Thermal Science and Engineering Applications, Nanotechnology Perceptions* Vol. 20 No.7 (2024)

DOI: 10.1115/1.4049703.

- 5. Jadhav P, Desai R, Patil M, Kulkarni S, "Thermal conductivity comparison of CuO-water nanofluids and CuO-TiO<sub>2</sub> hybrid nanofluids", Materials Today: Proceedings, DOI: 10.1016/j.matpr.2020.10.277.
- 6. Khan M, and Ahmad Z, "Stability and Agglomeration Behavior of Hybrid Nanofluids: A Comparative Study", Journal of Nanofluid Science and Engineering, Volume: 119, Issue: 1-2 pages:169-194, DOI:10.1007/s00170-022-08603-6.
- 7. Singh R, Kumar A, and Sharma P, "Synthesis and Performance Analysis of Cu-Graphene Hybrid Nanofluids for Optimizing Viscosity and Reducing Pressure Drop in Heat Transfer Systems", Journal of Thermal Analysis and Calorimetry. DOI: 10.1007/s10973-021-10545-9.
- 8. Kumar S, Patel R, Verma A, Singh P, "Thermal and Rheological Properties of Hybrid Nanofluids Containing Graphene Oxide and TiO<sub>2</sub>: A Comparative Analysis". Journal of Molecular Liquids, DOI: 10.1016/j.molliq.2021.117987.
- 9. Eastman, J. A. Choi, S. U. S., Li, S. Yu, W Thompson, L. J. "Enhanced Thermal Conductivity Through the Development of Nanofluids". Applied Physics Letters, DOI: 10.1063/1.1341218.
- 10. Esfe M, Saedodin S, Afrand M H, Rostamian H, "Thermal Conductivity Enhancement of Water Using Hybrid Nanofluids Comprising SiO<sub>2</sub> and TiO<sub>2</sub> Nanoparticles for Heat Transfer Applications". Journal of Thermal Science and Engineering Applications, DOI: 10.1115/1.4039781.
- 11. Suresh, S Kumar, V Rajan, S Patel, R. Impact of Density and Sedimentation on Heat Transfer Performance of Hybrid Nanofluids Containing Graphene Oxide and TiO<sub>2</sub> Nanoparticles, International Journal of Heat and Mass Transfer, DOI: 10.1016/j.ijheatmasstransfer.2020.120234.
- 12. Putra N, Rohaizar A, Aziz M, Enhanced Specific Heat Capacity of SiO<sub>2</sub>-TiO<sub>2</sub> Hybrid Nanofluids for Improved Energy Storage in Heat Exchangers, Journal of Energy Storage, DOI: 10.1016/j.est.2016.01.005.
- 13. Oztop H F, Koca A S, Aydin O, Thermal Properties of Hybrid Nanofluids Containing SiO<sub>2</sub> and TiO<sub>2</sub> for Natural Convection Applications, International Journal of Thermal Sciences, 10.1016/j.ijthermalsci.2015.06.018.